# Using a Liquid Xenon Positron Target


Max Varverakis* and Robert Holtzapple†
*California Polytechnic State University, San Luis Obispo, CA 93407, USA*

Spencer Gessner‡
*SLAC National Accelerator Laboratory, Menlo Park, California 94025, USA*

Hiroki Fujii§
*Nishina Center, RIKEN, 2-1 Hirosawa, Wako, Saitama, 351-0198, Japan*



(Dated: September 6, 2022)



Positron targets are a critical component of future Linear Colliders. Traditional targets are composed of high-Z metals and become brittle over time due to constant bombardment by high-power electron beams. We explore the possibility of a liquid Xenon target which is constantly refreshed and therefore not susceptible to the damage mechanisms of traditional solid targets. Using the GEANT4 simulation code, we examine the performance of the liquid Xenon target and show that the positron yield and divergence are comparable to solid targets when normalizing by radiation length. We develop parameter sets for a demonstration application at FACET-II and an ILC-type positron source.


## I. INTRODUCTION

For future Linear Collider applications, around $10^{14}$ $e^+$ per second need to be produced [1]. In addition to the quantity of positrons, they generally need to have a minimum energy based off of the design of the accelerator.

The traditional scheme for producing positrons is by colliding high energy electrons into a high-Z target. The collision between an electron beam and a target generates an electromagnetic particle shower producing positrons.

In order to generate $10^{14}$ $e^+$ per second, an extremely high-powered electron beam is required, which results in large power deposits in the target. Hence, solid targets tend to degrade over time [2].

Previous experiments have been carried out to explore alternatives to using solid targets, such as using liquid Mercury (Hg), but the apparent hazards that Hg presents limits its applications [3]. Other liquid targets have been investigated in the undulator scheme for ILC, such as Bi-Pb [3] and Pb [4]. Related studies include using liquid Lithium to generate neutrons from a proton beam [5], as well as using a gaseous deuterium target and positron beam for muon production [6].

In this paper, we explore the use of a liquid Xenon (LXe) target to produce positrons under the hypothesis that the liquid flow will be able to account for the power deposits discussed above. Figure 1, a basic schematic of the LXe target and beam interaction.

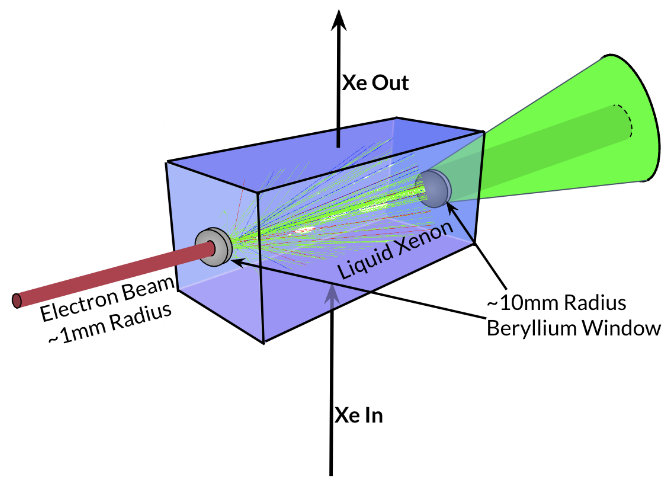


FIG. 1: Liquid Xenon target setup.

## II. SIMULATION RESULTS

Using GEANT4 [7], we compare our LXe target to a Tantalum (Ta) target due to previous experience with Tantalum positron targets at FACET-II[1] [8]. An incident electron energy of 10 GeV was chosen. We expect to see similar positron yields for both targets when normalizing by radiation lengths. Since the radiation length of liquid Xenon is around 7 times greater than that of Tantalum, the transverse spread of the positron shower should be larger in the liquid Xenon target. For practical purposes, other than for energy deposition considerations, we do not consider positrons on the exit of the target under 20 MeV and over 10 mm transverse displacement, which is


* mvarvera@calpoly.edu
† rholtzap@calpoly.edu
‡ sgess@slac.stanford.edu
§ hiroki.fujii@riken.jp


[1] We also simulated a Tungsten (W) target, but the results were similar enough to Ta that we did not include it in the comparison.

based off of similar positron acceptances in [9, 10]. See Table I for parameters used in the simulation.

| **Material** | **Symbol** | **Z** | **Density** $[\mathrm{g\cdot cm^{-3}}]$ | **Rad Length** [cm] |
|---|---|---|---|---|
| Tantalum | Ta | 73 | 16.654 | 0.4094 |
| Liquid Xe | LXe | 54 | 2.953 | 2.872 |

TABLE I: Parameters used in GEANT4 simulation when comparing targets.

To calculate the normalized RMS emittance of the positrons generated in pair production, we utilize the following [11]

$$\varepsilon_{n,rms} = \frac{1}{m_0 c}\sqrt{\langle x^2\rangle \langle p_x^2\rangle - \langle xp_x\rangle}. \quad (1)$$

At max positron yield, the transverse emittance for Ta is $\sim 9\mathrm{mm\cdot rad}$ while the transverse emittance for LXe is $\sim 36\mathrm{mm\cdot rad}$. According to [9, 10], the transverse emittance for LXe is comparable for use in Linear Colliders.

From Figure 2, the max positron yield for both Ta and LXe occurs at around 4.5 radiation lengths. Observe that both targets generate a similar yield distribution when normalizing by radiation lengths, as predicted. Despite having different radiation lengths, the energy of the positrons exiting the target are relatively equal for both target materials.

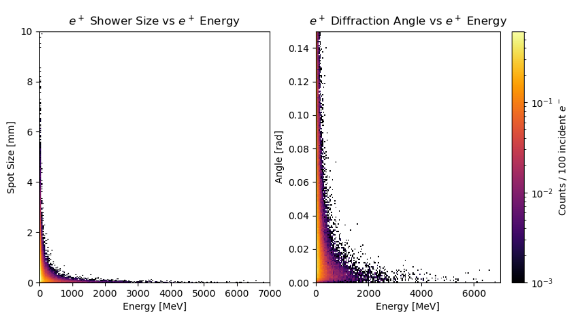


(a) Tantalum target.

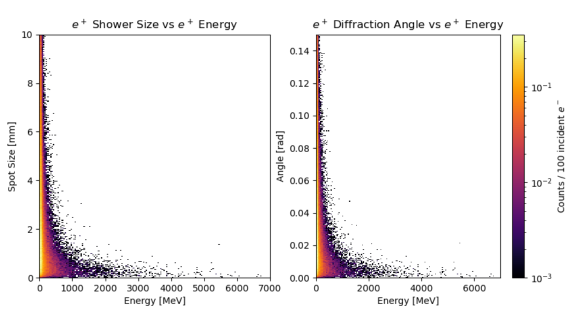


(b) Liquid Xenon target.

FIG. 3: Transverse displacement and angular diffraction of positrons as a function of their energy upon target exit. Data is shown for widths of 4.5 radiation lengths (max $e^+$ yield).

Notice that in Figure 3, the angular divergence of positrons is roughly the same for both targets, yet the transverse widths are more broadly distributed for the liquid Xenon target. This can be explained by the fact that the radiation length of LXe is roughly seven times that of Tantalum.

In simulation, we compare the energy deposited in the target for both materials per incident $e^-$. Although these deposits seem large, as we indicate in Section III A, the flow of LXe can take into account the energy deposit without much concern.

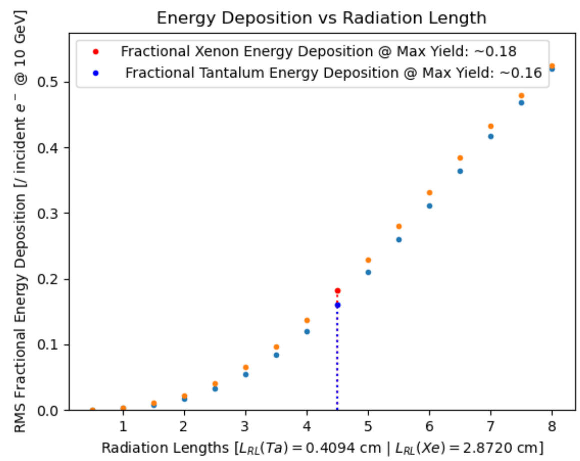


FIG. 4: Energy deposition in Ta and LXe targets per incident electron at 10 GeV.

## III. CRYO-COOLED LIQUID XENON CHAMBER

### A. Calculating the Liquid Xenon Flow Rate

To calculate the flow rate of the LXe, we first calculate preliminary values using the information given in Table II. To see resultant quantities, seek Table III.

| **Liquid Xenon** | **Symbol** | **Value** | **Units** |
|---|---|---|---|
| Molar Mass | M | 131.293 | u |
| Density | $\rho$ | 2.953 | $\mathrm{g\cdot cm^{-3}}$ |
| Vapor Pressure | $p$ | 300 | kPa |
| Heat of Vaporization | $\Delta$H | 12.636 | $\mathrm{kJ\cdot mol^{-1}}$ |
| Heat of Vap./Volume | $\Delta\mathrm{H_{vol}}$ | 284.205 | $\mathrm{J\cdot cm^{-3}}$ |
| Radiation Length | $\mathrm{L_{RL}}$ | 2.872 | cm |
| Width | $\frac{\mathrm{d}}{\mathrm{L_{RL}}}$ | 4.5 | $\mathrm{L_{RL}}$ |

TABLE II: Important parameters associated with LXe target chamber.

We first convert the heat of vaporization to units of energy per unit volume ($\mathrm{J\cdot cm^{-3}}$),

$$\Delta\mathrm{H_{vol}} = \frac{\Delta\mathrm{H}\cdot\rho}{\mathrm{M}}. \quad (2)$$

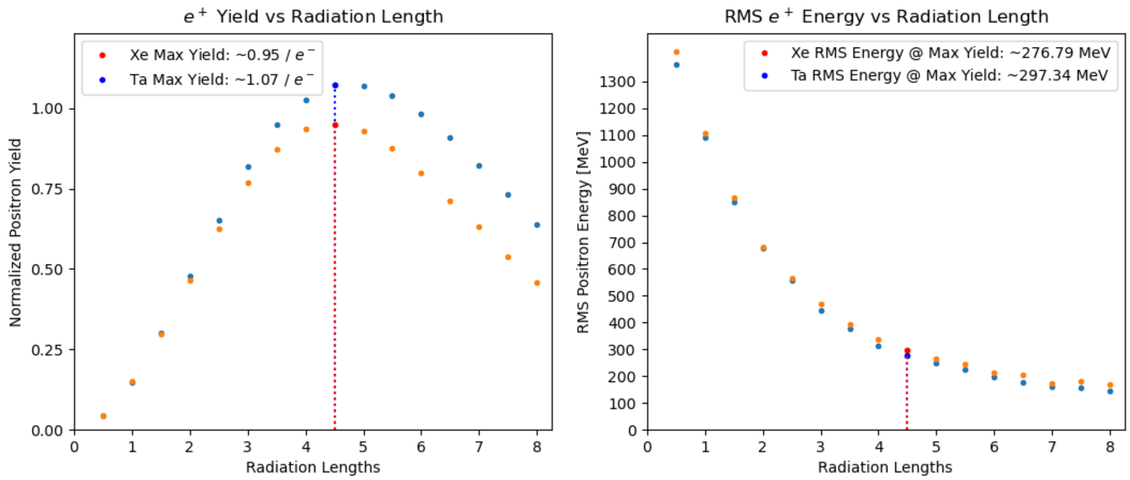


FIG. 2: Positron yield and RMS energy upon exiting the target per incident $e^-$ at 10 GeV.

| **Beam Parameters** | **Symbol** | **FACET-II** [12] | **ILC** [1] | **Units** |
|---|---|---|---|---|
| Energy | $E$ | 10.0 | 6.0 | GeV |
| Repetition Rate | $f$ | 10 | 300 | Hz |
| Charge | $q$ | 2 | 3.204 | nC |
| Number of $e^-$ | n | 1.248 | 2.0 | $10^{10}$ |
| **Resultant Quantities** | | | | |
| Energy Deposition/$e^-$ | $\mathrm{E_{dep}}$ | 1.9 | | GeV |
| Energy Deposit/Pulse | $\epsilon$ | 3.8 | 482.1 | J |
| Peak Energy Deposit Density | $\epsilon_\rho$ | $1.96 \times 10^{-2}$ | 15.22 | $\mathrm{J{\cdot}g^{-1}}$ |
| Power Deposit/Pulse | $P_{\mathrm{dep}}$ | 38.0 | $1.45 \times 10^5$ | W |
| Flow Rate due to Vaporization | Q | 0.134 | 508.9 | $\mathrm{cm^3 \cdot s^{-1}}$ |
| Main Shower Path Flow Rate | $Q_{\mathrm{vol}}$ | 0.5170 | 15.51 | $\mathrm{L{\cdot}s^{-1}}$ |

TABLE III: Linear collider electron beam parameters and associated target quantities.

Then, one can calculate the number of electrons per beam bunch, by comparing the total charge of the beam bunch to the charge of an electron ($e \approx 1.602 \times 10^{-10}$ nC). From this, we calculate the total energy deposited in the LXe target. We can obtain the flow rate of LXe required to replace the vaporized Xenon due to the energy deposited by the beam,

$$Q = \frac{\epsilon \cdot f}{\Delta \mathrm{H_{vol}}}. \tag{3}$$

In case one wants to calculate the flow rate required to move the entire volume encompassing the main part of the EM shower, the volume can be approximated with a rectangular prism with target width and side lengths equal to the diameter of the Beryllium windows (see next section). At max positron yield, this gives $\mathrm{V} = (2\ \mathrm{cm})^2 \cdot 4.5\mathrm{L_{RL}} \approx 51.70\ \mathrm{cm}^3$. As a result, the required flow rate to move volume V in the amount of time between beam pulses is shown in Table III as $Q_{\mathrm{vol}}$.

### B. Using Beryllium Windows to the Target Chamber

We explore using Beryllium (Be) windows for the beam to enter and exit the target chamber.

| Beryllium | Symbol | Value | Units |
|---|---|---|---|
| Atomic Number | Z | 4 | |
| Density | $\rho$ | 1.844 | g·cm$^{-3}$ |
| Rupture Modulus | $F_a$ | 400 | MPa |
| **Quantities** | | | |
| Height | $h$ | 1.0 | m |
| Radius | $r$ | 10.00 | mm |
| Contact Area | $A$ | $100\pi$ | mm$^2$ |
| Pressure | $P$ | 328.968 | kPa |
| Force | $F$ | 9.100 | N |
| Safety Factor | $S_F$ | 4 | |
| Empirical Constant | $K$ | 0.75 | |
| Thickness | $T$ | 147.395 | $\mu$m |

TABLE IV: Useful quantities and properties of solid Beryllium. The quantities are specific to a 10mm radius Beryllium disk.

Utilizing Bernoulli's Equation for conservative force fields, we can calculate the total pressure on a Be window. However, as seen in Table III, the flow rate for the LXe is quite small, so we can approximate the pressure to be

$$P = \rho g h + p, \tag{4}$$

where $g$ is acceleration due to gravity, $h$ is the height of the Xenon chamber relative to the height of the window, and $p$ is the additional pressure (in this case $p$ refers to the vapor pressure of LXe $\sim$ 300kPa). From Eq. (4), we can calculate the force on a Be window with contact area $A$ by multiplying the area by the pressure.

In order to determine the required thickness of the Be windows, we utilize methods described in [13]. First we calculate a constant related to the safety factor of our thickness, which takes into account the method with which the Be window is inserted into the target chamber. An empirical constant $K = 0.75$ is chosen if the window is clamped into the target chamber, and $K = 1.125$ if the window is unclamped in the target chamber. For a given safety factor ($S_F$), we have a thickness of

$$T = r \cdot \sqrt{\frac{S_F \cdot K \cdot P}{F_a}}. \tag{5}$$

For parameters chosen in Table IV, we get a required thickness of 496.701$\mu$m. Using the above thickness, we simulated the energy deposited in both of the Be windows, and found that the energy deposited in the entrance window is on the order of $10^{-1}$ MeV/incident $e^-$ and the exit window on the order of 6 MeV/incident $e^-$.

**TODO** Explore how much heat Be windows can take in given amount of time like done above for LXe?? Energy transfer from windows to LXe??

## IV. CONCLUSION

### A. Design of Liquid Xenon Chamber

Source code and sample data from GEANT4 simulations can be found at `https://github.com/MaxVarverakis/LiquidXenonSims.git`.


[1] Y. Seimiya, M. Kuriki, T. Takahashi, T. Omori, T. Okugi, M. Satoh, J. Urakawa, and S. Kashiwagi, Positron capture simulation for the ILC electron-driven positron source, Progress of Theoretical and Experimental Physics **2015**, 103G01 (2015).

[2] V. Bharadwaj, Y. Batygin, J. Sheppard, D. Schultz, S. Bodenstein, J. Gallegos, R. Gonzales, J. Ledbetter, M. Lopez, R. Romero, T. Romero, R. Rutherford, and S. Maloy, Analysis of beam-induced damage to the slc positron production target, in *PACS2001. Proceedings of the 2001 Particle Accelerator Conference (Cat. No.01CH37268)*, Vol. 3 (2001) pp. 2123–2125 vol.3.

[3] A. A. Mikhailichenko, Liquid metal target for ilc, in *Proceedings of EPAC 2006, Edinburgh, Scotland* (2006).

[4] J. C. Sheppard, *Liquid Metal Target for NLC Positron Source*, Tech. Rep. (2002).

[5] G. Feinberg, M. Paul, A. Arenshtam, D. Berkovits, Y. Eisen, M. Friedman, S. Halfon, D. Kijel, A. Nagler, A. Shor, and I. Silverman, A liquid-lithium target project for production of high-intensity quasi-stellar neutrons, in *Proceedings of 11th Symposium on Nuclei in the Cosmos — PoS(NIC XI)* (Sissa Medialab, 2011).

[6] H. Okita, Y. Ishi, and Y. Mori, Beam emittance growth in the proposed gaseous target ERIT ring for muon production, Nuclear Instruments and Methods in Physics Research Section A: Accelerators, Spectrometers, Detectors and Associated Equipment **982**, 164565 (2020).

[7] S. Agostinelli *et al.* (GEANT4), GEANT4–a simulation toolkit, Nucl. Instrum. Meth. A **506**, 250 (2003).

[8] H. Fujii, K. Marsh, W. An, S. Corde, M. Hogan, V. Yakimenko, and C. Joshi, Positron beam extraction from an electron-beam-driven plasma wakefield accelerator, Physical Review Accelerators and Beams **22**, 10.1103/physrevaccelbeams.22.091301 (2019).

[9] H. Tang, A. Kulikov, J. Clendenin, S. Ecklund, R. Miller, and A. Yeremian, The NLC positron source, in *Proceedings Particle Accelerator Conference* (IEEE, 1995).

[10] J. Sheppard, *Conventional Positron Target for a Tesla Formatted Beam(LCC-0133)*, Tech. Rep. (2003).

[11] K. Floettmann, Some basic features of the beam emittance, Physical Review Special Topics - Accelerators and Beams **6**, 10.1103/physrevstab.6.034202 (2003).

[12] N. G. Author, *Technical Design Report for the FACET-II Project at SLAC National Accelerator Laboratory*, Tech. Rep. (2016).

[13] C. Ltd, *The CRYSTRAN HANDBOOK of Infra-Red and Ultra-Violet OPTICAL MATERIALS* (2019).